

DETECTION OF NUCLEAR X-RAY SOURCES IN NEARBY GALAXIES WITH *CHANDRA*

LUIS C. HO¹, ERIC D. FEIGELSON², LEISA K. TOWNSLEY², RITA M. SAMBRUNA^{2,3},
GORDON P. GARMIRE², W. N. BRANDT², ALEXEI V. FILIPPENKO⁴, RICHARD E. GRIFFITHS⁵,
ANDREW F. PTAK⁵, AND WALLACE L. W. SARGENT⁶

To appear in The Astrophysical Journal (Letters).

ABSTRACT

We report preliminary results from an arcsecond-resolution X-ray survey of nearby galaxies using the Advanced CCD Imaging Spectrometer (ACIS) on board the *Chandra X-ray Observatory*. The total sample consists of 41 low-luminosity AGNs, including Seyferts, LINERs, and LINER/H II transition objects. In the initial subsample of 24 objects observed thus far, we detect in $\sim 62\%$ of the objects a compact, point-like source astrometrically coincident with either the optical or radio position of the nucleus. The high detection rate strongly suggests that the majority of the objects do contain weakly active, AGN-like cores, presumably powered by central massive black holes. The 2–10 keV luminosities of the nuclear sources range from $< 10^{38}$ to 10^{41} erg s⁻¹, with a median value of 2×10^{38} erg s⁻¹. Our detection limit corresponds to $L_X(2\text{--}10 \text{ keV}) \approx 8 \times 10^{37}$ erg s⁻¹ for the typical sample distance of 12 Mpc; this limit is two orders of magnitude fainter than the weakest sources of this kind previously studied using *ASCA* or *BeppoSAX*. The new data extend toward lower luminosities the known linear correlation between hard X-ray and H α luminosity for broad-line AGNs. Many narrow-line objects do contain X-ray cores, consistent with either weak AGNs or X-ray binary systems, but they have X-ray luminosities a factor of 10 below the $L_X\text{--}L_{H\alpha}$ relation of the broad-line sources. Their distributions of photon energies show no indication of exceptionally high absorption. The optical line emission in these nuclei is likely powered, at least in part, by stellar processes.

Subject headings: galaxies: active — galaxies: nuclei — galaxies: Seyfert — X-rays: galaxies

1. INTRODUCTION

Knowledge of the local space density of active galactic nuclei (AGNs) impacts many astrophysical issues. Surveys for nearby AGNs furnish critical data for quantifying the faint end of the AGN luminosity function, for characterizing the demography of massive black holes, and for investigating accretion physics. Optical spectroscopic surveys indicate that many nearby galaxies possess mildly active nuclei (Ho, Filippenko, & Sargent 1997b). Although a significant fraction of these objects do contain accretion-powered sources qualitatively similar to more powerful AGNs such as classical Seyfert nuclei and quasars (Ho 1999), the physical nature of many still remains ambiguous. Observations at ultraviolet and optical wavelengths sometimes point to stellar processes as the underlying agent responsible for the activity (e.g., Maoz et al. 1998; Barth & Shields 2000), but these data generally cannot rule out the presence of a highly obscured AGN component.

Unless Compton-thick conditions prevail, hard X-ray data provide a much more definitive probe. In recent years, observations using *ASCA* and *BeppoSAX* have shed considerable light on the nature of low-luminosity AGNs (see Terashima 1999 and Ptak 2001 for reviews). The fairly coarse angular resolution of these satellites, however, has biased detections to more luminous sources which are less

contaminated by extended emission from the host galaxy. Moreover, the relatively long integration times required for the observations necessarily restricted the published studies to small, usually X-ray selected, and possibly unrepresentative samples.

The exquisite imaging capability of the *Chandra X-ray Observatory* offers significant advantages for the study of low-luminosity AGNs. The good instrumental response for photon energies up to 8 keV permits detection of faint AGN emission even if subject to absorption as high as $N_H \approx 10^{24}$ cm⁻². Thus, obscured AGNs can be found. Faint nuclei embedded deeply in the central regions of bright bulges can be detected reliably only under high angular resolution. As we demonstrate in this Letter, *Chandra* can probe the nuclear regions of nearby galaxies effectively and efficiently, allowing us to survey, for the first time, a sizable sample of optically selected galaxies covering a wide range of nuclear activity. With brief, “snapshot” exposures, we are able to detect or set stringent limits to compact nuclear X-ray sources with unprecedented sensitivity. We revisit some longstanding, unresolved issues concerning the physical nature of low-luminosity AGNs in light of the new measurements. The sharp X-ray images additionally reveal a plethora of previously unknown structural details in the circumnuclear

¹The Observatories of the Carnegie Institution of Washington, 813 Santa Barbara St., Pasadena, CA 91101-1292.

²Department of Astronomy and Astrophysics, The Pennsylvania State University, 525 Davey Lab, University Park, PA 16802.

³George Mason University, Department of Physics and Astronomy, MS 5C3, Fairfax, VA 22030-4444.

⁴Department of Astronomy, University of California, Berkeley, CA 94720-3411.

⁵Department of Physics, Carnegie Mellon University, 5000 Forbes Ave., Pittsburgh, PA 15213.

⁶Palomar Observatory, 105-24 Caltech, Pasadena, CA 91125.

TABLE 1: *Chandra* OBSERVATIONS OF LOW-LUMINOSITY AGNs

TARGET GALAXIES					X-RAY PROPERTIES						
NGC	D (Mpc)	Hubble Type	Spectral Class	$\log L_{H\alpha}$ (erg s^{-1})	Exp. (ks)	ACIS Flags	Nucleus Position	Counts	$\log L_X$ (erg s^{-1})	X-ray Class	Notes
(1)	(2)	(3)	(4)	(5)	(6)	(7)	(8)	(9)	(10)	(11)	(12)
1055	12.6	SBb:	T2:	37.92	1.1	a	O	<3	<38.19	IV	...
1058	9.1	Sc	S2	38.16	2.4	a	O	<3	<37.57	IV	...
2787	7.5	SB0+	L1.9	38.71	1.2	a, b	O	7	38.31	III	...
2841	12.0	Sb:	L2	38.80	1.7	a	R	6	38.26	II	a
3031 (M81)	3.6	Sab	S1.5	38.94	2.4	...	R	21000	40.20	I	b, c
3486	7.4	SABc	S2	37.85	1.8	...	O	<3	<37.51	IV	...
3489	12.1	SAB0+	T2	38.48	1.8	b	O	11	38.23	II	d
3627	10.3	SABb	T2	39.35	1.8	...	R	<3	<37.61	IV	e
3628	10.3	Sb pec	T2	37.43	1.8	...	R	<3	<37.68	IV	f, c
3675	12.8	Sb	T2	38.22	1.8	b	O	<3	<37.99	IV	...
4203	15.1	SAB0-	L1.9	38.98	1.8	...	R	410	40.08	I	g, c
4278 (M98)	16.1	E1+	L1.9	39.60	1.4	c	R	310	40.09	I	...
4321 (M100)	16.1	SABbc	T2	39.35	6.5	b	R	<26	<38.59	II or IV	h
4374 (M84)	18.4	E1	L2	39.35	3.1	c	R	37	39.12	III	i, c
4395	2.6	Sm:	S1.8	38.53	1.2	...	R	112	38.50	I	c
4494	17.1	E1+	L2:	<37.79	1.8	a, b	O	22	38.86	I	...
4569 (M90)	16.8	SABab	T2	40.28	1.7	...	R	43	39.41	II	j, c
4579 (M58)	16.8	SABb	S1.9	39.72	4.1	d	R	3600	40.95	I	k, c
4594 (M104)	9.8	Sa	L2	39.48	1.8	a, d	R	350	40.14	I	l, c
4639	22.9	SABbc	S1.0	39.90	1.4	c	R	290	40.45	II	m, c
4725	13.0	SABab pec	S2:	38.24	1.7	a	O	43	39.16	II	n
4826 (M64)	7.5	Sab	T2	39.13	1.8	...	R	<12	<37.86	II or IV	o
5033	18.7	Sc	S1.5	40.42	2.9	c	R	1200	40.71	I	c
5195	7.7	I0 pec	L2:	38.59	1.1	a	O	<3	<37.85	IV	...

NOTE.— Col. (1) Galaxy name. Col. (2) Adopted distance, mostly based on observations of Cepheid stars (Ferrarese et al. 2000) and surface-brightness fluctuations (Tonry et al. 2001), and otherwise from Tully 1988, who assumes $H_0 = 75 \text{ km s}^{-1} \text{ Mpc}^{-1}$. Col. (3) Hubble type. Col. (4) Spectral class of the nucleus, where L = LINER, S = Seyfert, T = “transition object” (LINER/H II), 1 = type 1, 2 = type 2, and a fractional number between 1 and 2 denotes various intermediate types; uncertain and highly uncertain classifications are followed by a single and double colon, respectively. Col. (5) Extinction-corrected $H\alpha$ luminosity (narrow + broad components). Data for cols. (3)–(5) taken from Ho et al. 1997a and Ho et al. 1997c, with the $H\alpha$ luminosities updated to reflect the distances in col. (2). Col. (6) ACIS effective exposure time, corrected for losses during readout. Col. (7) ACIS flags: (a) aspect suffered $\approx 8'$ offset; (b) aspect aligned with USNO counterpart; (c) 1/2-chip subarray mode used to reduce pile-up; (d) 1/8-chip subarray mode used to reduce pile-up. Col. (8) Nucleus position: O = optical position from Palomar Sky Survey ($\approx 2''$ accuracy); R = radio interferometric position (<0.3 accuracy). Col. (9) Counts from nucleus in 0.2–8 keV band. Col. (10) Intrinsic X-ray luminosity in the 2–10 keV band. Col. (11) X-ray morphology class (see Fig. 1). Col. (12) Notes: (a) Crowded field with ~ 100 counts in a $30'$ -diameter region around the nucleus comprised of a dozen sources mostly concentrated $6'$ E of the VLA source. We tentatively associate the ~ 6 counts $2'$ NE of the VLA position with the nucleus, as this offset is consistent with typical errors in the *Chandra* aspect solution. (b) This strong nuclear source is heavily piled up. The ACIS counts are estimated from the readout trail. (c) Observed with *ASCA*. (d) Crowded field with ~ 25 counts in a $5'$ -diameter region around the nucleus comprised of ~ 4 sources. (e) Crowded field. The nucleus may be present with ~ 2 counts. (f) Crowded field with uncertain position for the nucleus, which may be present with a few counts. (g) X-ray emission extends to the SE of the nucleus. (h) Crowded field. Although the X-ray field astrometry is accurate, the position of the nucleus is uncertain. The nucleus could be associated with a 26-count source (giving the listed upper limit) or a 4-count source, or it could be undetected with <3 counts. (i) While the extended X-ray emission of M84 is well known, the clearly resolved nucleus is new here. The diffuse emission shows a strong asymmetric enhancement $\sim 30'$ to the SE which may result from interaction of the radio jets with the hot interstellar medium. (j) Crowded field with 71 counts in a $10'$ -diameter region. (k) Weak diffuse emission extends over a $40'$ -diameter region around the bright nucleus. (l) Crowded field along the edge-on disk of the “Sombrero” galaxy. (m) Crowded field over $8'$ -diameter region. (n) An extremely soft X-ray source (most photons with energies below 0.5 keV) with a $2'$ NS extent is present centered $3'$ SW of the position of the nucleus. We tentatively associate this source with the nucleus. (o) Crowded field with 70 counts in a $13'$ -diameter region. With uncertain astrometry, it is unclear whether the nucleus is detected at a level up to 12 counts (giving the listed upper limit), or is undetected with <3 counts.

environment of nearby galaxies.

2. OBSERVATIONS AND DATA ANALYSIS

Our targets were selected from the Palomar survey of nearby galaxies, a sensitive spectroscopic study of a nearly complete sample of 486 bright ($B_T \leq 12.5$ mag), northern ($\delta > 0^\circ$) galaxies (Ho, Filippenko, & Sargent 1997a,b). As part of the Guaranteed Observer program for the Advanced CCD Imaging Spectrometer (ACIS; Garmire et al. 2001) team, we chose a sample of 41 emission-line nuclei considered to be AGN candidates, including Seyfert nuclei, low-ionization nuclear emission-line regions (LINERs; Heckman 1980), and LINER/H II “transition” nuclei (Ho et al. 1997b). Thirty-five objects belong to a complete, volume-limited sample within 13 Mpc; the remaining were included as prototypes of different classes. To date, observations have been acquired for 24 galaxies. While this subsample is at the moment somewhat heterogeneous, it does form a representative subset of nearby objects with weak nuclear activity, and it covers a mixture of Hubble types. The sample, summarized in Table 1, is equally divided among Seyferts, LINERs, and transition objects; of these, 1/3 are “type 1” and 2/3 are “type 2” sources, nuclei with and without evidence for broad emission lines,

respectively. The median distance is 12 Mpc.

Each galaxy was observed with ACIS on board *Chandra* (Weisskopf, O’Dell, & van Speybroeck 1996). We used the on-axis backside-illuminated CCD chip in the spectroscopic array because it is more sensitive to soft (0.2 keV $< E < 0.5$ keV) X-rays than the frontside-illuminated chips in the imaging array. Most observations used the standard mode of reading out the full chip every 3.2 s, but in six cases where a bright nuclear source was known from *ROSAT* or *ASCA* studies, only a portion of the chip was read out more frequently in order to reduce photon pile-up. Exposures of 2 ks were requested, but the actual integrations ranged from 1.1 to 6.5 ks due to constraints on satellite scheduling.

Our treatment of the data starts with the Level 1 event file produced by the *Chandra* X-ray Center. We first apply a correction for charge-transfer inefficiency which reduces biases in event energies and grades (Townsend et al. 2000). Next, the data are cleaned of events with bad status flags, hot columns, and bad flight grades from cosmic-ray impacts. We then select *ASCA* grades 02346 and energies 0.2–8 keV for science analysis. A search for sources is conducted in both the target and ancillary CCD chips using a wavelet-transform algorithm for source detection (Freeman et al. 2001). Unresolved on-axis sources can be

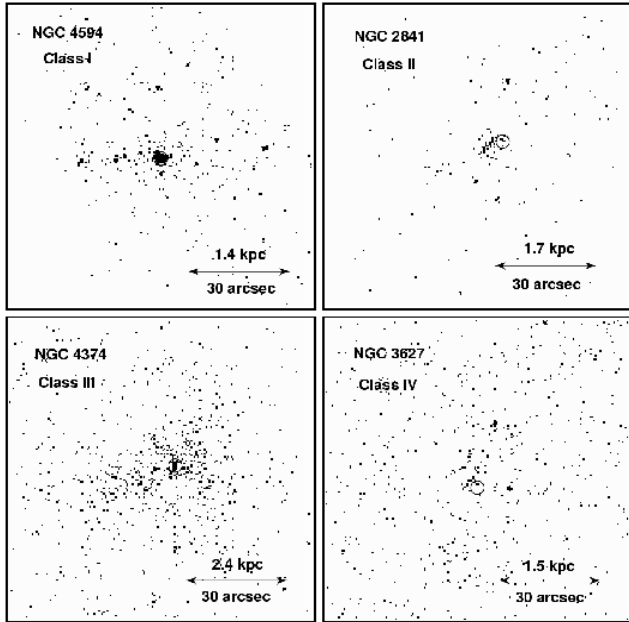


FIG. 1.— Representative ACIS images of the inner regions of nearby galaxies hosting low-luminosity AGNs, chosen to exemplify the four X-ray classes: I = dominant nucleus; II = nucleus comparable in brightness to off-nuclear sources in the galaxy; III = nucleus embedded in diffuse emission; and IV = nucleus absent. Each panel subtends $90'' \times 90''$, and the $4''$ -diameter circle is centered on the radio or optical position of the nucleus.

reliably located as faint as $\simeq 4$ counts. Nuclear counts were typically extracted from a $2''$ -diameter circle without background subtraction, but certain cases required special treatment (see notes to Table 1). ACIS count rates are converted to X-ray luminosities assuming an intrinsic power-law spectrum with photon index $\Gamma = 1.8$ and absorption from our Galactic interstellar medium with column density $N_{\text{H}} = 2 \times 10^{20} \text{ cm}^{-2}$. These assumptions⁷ give $L_{\text{X}}(2\text{--}10 \text{ keV}) = 3.6 \times 10^{37} \text{ erg s}^{-1} (\text{ACIS cts/ks}) (D/10 \text{ Mpc})^2$. We quote X-ray luminosities in the 2–10 keV range for ease of comparison with literature data.

Examination of the images quickly revealed that, in many cases, the nucleus is only one, and not necessarily the brightest, of many X-ray sources or structures in the core regions of the target galaxies. Astrometric alignment of the X-ray image to the galaxy is thus critical. The satellite aspect system based on star-tracker cameras gives absolute astrometric alignments in the *Hipparcos* frame with accuracies usually within $\pm 2''$. But in a few cases, X-ray sources unrelated to the galaxy are found to be associated with foreground stars ($R \simeq 10\text{--}15 \text{ mag}$) with positions from the USNO A-2 catalog accurate to $\pm 0''.3$. For most of the target galaxies, the location of the nucleus is known to high accuracy ($\pm 0''.3$ and often $< 0''.1$) from radio observations. But for some, no radio source is found, and positions are based on relatively inaccurate measurements from sky survey Schmidt plates (around $\pm 2''$). Thus, our ability to align the ACIS image to the galaxy ranges from a few tenths to several arcseconds. A more detailed discussion of the X-ray analysis will be presented for the full volume-limited sample in a forthcoming paper.

⁷The hard X-ray spectra of most low-luminosity AGNs are well fit by $\Gamma \approx 1.8$, and in many cases no significant absorption in excess of the Galactic foreground is indicated (e.g., Terashima 1999). None of our objects suffer heavy Galactic extinction; the median $N_{\text{H}} \approx 2 \times 10^{20} \text{ cm}^{-2}$. The luminosities would increase by a factor of 1.8 and 6.7 for intrinsic columns of 2×10^{21} and $2 \times 10^{22} \text{ cm}^{-2}$, respectively.

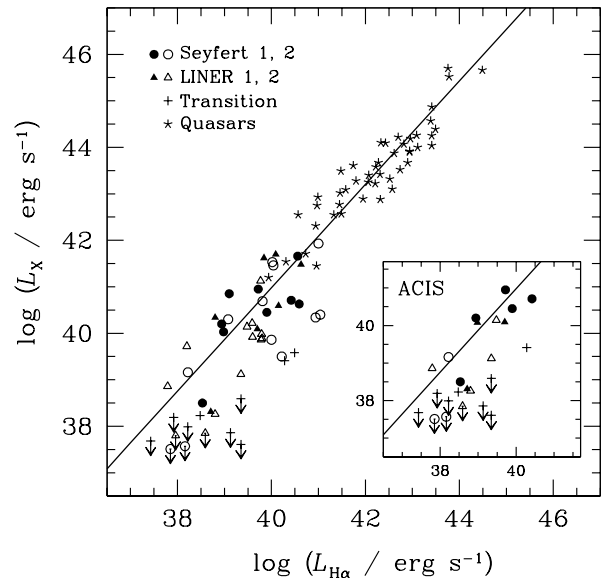


FIG. 2.— The $L_{\text{X}}\text{--}L_{\text{H}\alpha}$ correlation for AGNs. The X-ray luminosity represents the intrinsic (unabsorbed) power-law component in the 2–10 keV band. The $\text{H}\alpha$ luminosity includes both the narrow and broad (if present) components of the line, corrected for extinction due to the Galaxy and the narrow-line region. The data for low- z quasars are taken from Ward et al. (1988), adjusted to $H_0 = 75 \text{ km s}^{-1} \text{ Mpc}^{-1}$. The low-luminosity sources (low-luminosity Seyferts, LINERs, and transition nuclei) come from this paper and Terashima et al. (2000a), whose distances have been updated according to the precepts outlined in Table 1. The *solid line* shows the best-fit unweighted linear regression line (see text) for the type 1 objects and low- z quasars. The insert on the lower right corner of the graph highlights the new ACIS observations for clarity.

3. RESULTS AND DISCUSSION

The morphologies of the X-ray images can be loosely grouped into four classes (Fig. 1): (I) dominant nuclear source; (II) nuclear source comparable in brightness to off-nuclear sources in the galaxy; (III) nuclear source embedded in diffuse emission; and (IV) no nuclear source. A compact X-ray source can be associated with the optical or radio nucleus in 62% (15/24) of the galaxies. It is of interest to compare the detection frequency as a function of AGN spectral type. All eight of the broad-line nuclei (3 LINER 1s, 5 Seyfert 1s) were detected, by contrast to only 44% (7/16) of the narrow-line sources (1/3 Seyfert 2s, 4/5 LINER 2s, 2/8 transition objects). For LINERs as a class, the detection rate ranges from $\sim 60\%$ to $\sim 90\%$, depending on whether we include or exclude transition objects as LINERs.

The gross properties of the optical emission-line spectra of AGNs can be explained by photoionization from the central AGN continuum. In support of this picture, the strength of the hydrogen recombination lines generally scales with the X-ray luminosity in powerful Seyfert 1 nuclei and quasars (e.g., Kriss, Canizares, & Ricker 1980; Ward et al. 1988). The $L_{\text{X}}\text{--}L_{\text{H}\alpha}$ correlation has been shown to extend down to the regime of low-luminosity AGNs, both in the soft X-ray band (Koratkar et al. 1995; Roberts & Warwick 2000; Halderson et al. 2001) and in the hard X-ray band (Terashima, Ho, &

Ptak 2000a)⁸. This is consistent with the idea that low-luminosity AGNs share the same basic physical processes as in high-luminosity AGNs. Terashima et al. (2000a,b) find, however, that type 2 sources generally show systematically lower values of $L_X/L_{H\alpha}$ compared to type 1 objects.

Our sample reinforces these conclusions, as shown in Figure 2. Low-luminosity Seyfert 1s and LINER 1s trace the $L_X-L_{H\alpha}$ relation to $\log L_X \approx 38.5$, with a median $L_X/L_{H\alpha}$ of 15; the slope is close to, but slightly steeper than, unity. The best-fit unweighted linear regression line, calculated using the ordinary least-squares solution bisector with jackknife resampling (Feigelson & Babu 1992), for type 1 objects (including low- z quasars) is $\log L_X = (1.11 \pm 0.054) \log L_{H\alpha} - (3.50 \pm 2.27)$. The detected type 2 objects loosely follow the same correlation, but with somewhat greater scatter and offset toward lower $L_X/L_{H\alpha}$ (median ~ 2). The ACIS observations contribute nine stringent upper limits in the regime $\log L_X \lesssim 38.0$, all of which deviate significantly from the correlation established by the type 1 sources (most have $L_X/L_{H\alpha} < 1$). The majority of the upper limits are transition objects.

Note that the intrinsic scatter in the $L_X-L_{H\alpha}$ relation should be significantly less than indicated in Figure 2. The photometric errors associated with the luminosities for any individual object may be substantial (see footnote 7 for L_X and Ho et al. 1997a for $L_{H\alpha}$). The non-simultaneity of the X-ray and optical observations likely introduces additional scatter. Although the variability characteristics of low-luminosity AGNs are poorly constrained, some of them do vary, at least in the X-rays (e.g., Ptak et al. 1998). The $H\alpha$ measurements of Ho et al. (1997a) were extracted from a $2'' \times 4''$ aperture, somewhat larger than that used for the X-rays, but the effect of aperture mismatch should be minimal because the optical line emission tends to be highly centrally concentrated (Pogge et al. 2000).

The present sample is still small and incomplete, and we caution against premature generalizations based on the above statistics. Nonetheless, these early results are in broad agreement with the following:

(1) Most, perhaps all, low-luminosity type 1 objects, both Seyferts and LINERs, are genuine AGNs similar to classical Seyfert 1 nuclei and quasars.

(2) A significant fraction of low-luminosity type 2 sources do contain a central X-ray core, consistent with the presence of an AGN, but they are underluminous in X-rays compared to type 1 nuclei of the same $H\alpha$ luminosity. This suggests that the optical line emission may not be powered exclusively by a central AGN. Although detailed spectral fitting was not performed, examination of the photon energies indicates that few, if any, of the nuclear sources are absorbed by columns in the range $N_H \approx 10^{22} - 10^{24} \text{ cm}^{-2}$. Our data thus tentatively suggest that the standard unified model for Seyferts (Antonucci 1993) may not hold at very low luminosities. But we cannot exclude the presence of spectral components with $N_H \gtrsim 10^{25} \text{ cm}^{-2}$, nor the possibility that the X-ray emission in these systems arises entirely from X-ray binaries without any AGN component.

(3) Most transition objects are unrelated to AGNs.

(4) At least 60% of LINERs contain AGNs, consistent with the estimates of Ho (1996, 1999).

This work was sponsored by NASA contract NAS 8-38252 (Garmire, PI). The research of L. C. H. and A. V. F. is partly funded by NASA LTSA grant NAG 5-3556, and by NASA grants GO-06837.01-95A, AR-07527.02-96A, and AR-08361.02-97A from the Space Telescope Science Institute (operated by AURA, Inc., under NASA contract NAS5-26555). W. N. B. acknowledges support from NASA LTSA grant NAG 5-8107.

REFERENCES

- Antonucci, R. R. J. 1993, *ARA&A*, 31, 473
 Barth, A. J., & Shields, J. C. 2000, *PASP*, 112, 753
 Feigelson, E. D., & Babu, G. J. 1992, *ApJ*, 397, 55
 Ferrarese, L., et al. 2000, *ApJS*, 128, 431
 Freeman, P. E., Kashyap, V., Rosner, R., & Lamb, D. Q. 2001, *ApJ*, submitted
 Garmire, G. P., et al. 2001, in preparation
 Halderson, E. L., Moran, E. C., Filippenko, A. V., & Ho, L. C. 2001, *AJ*, submitted
 Heckman, T. M. 1980, *A&A*, 87, 152
 Ho, L. C. 1996, in *The Physics of LINERs in View of Recent Observations*, ed. M. Eracleous et al. (San Francisco: ASP), 103
 ——. 1999, *Adv. Space Res.*, 23 (5-6), 813
 Ho, L. C., Filippenko, A. V., & Sargent, W. L. W. 1997a, *ApJS*, 112, 315
 ——. 1997b, *ApJ*, 487, 568
 Ho, L. C., Filippenko, A. V., Sargent, W. L. W., & Peng, C. Y. 1997c, *ApJS*, 112, 391
 Koratkar, A. P., Deustua, S., Heckman, T. M., Filippenko, A. V., Ho, L. C., & Rao, M. 1995, *ApJ*, 440, 132
 Kriss, G. A., Canizares, C. R., & Ricker, G. R. 1980, *ApJ*, 242, 492
 Maoz, D., Koratkar, A. P., Shields, J. C., Ho, L. C., Filippenko, A. V., & Sternberg, A. 1998, *AJ*, 116, 55
 Pogge, R. W., Maoz, D., Ho, L. C., & Eracleous, M. 2000, *ApJ*, 532, 323
 Ptak, A. 2001, *Astro. Let. and Comm.*, in press (astro-ph/0008459)
 Ptak, A., Yaqoob, T., Mushotzky, R., Serlemitsos, P., & Griffiths, R. 1998, *ApJ*, 501, L37
 Roberts, T. P., & Warwick, R. S. 2000, *MNRAS*, 315, 98
 Terashima, Y. 1999, *Adv. Space Res.*, 23 (5-6), 851
 Terashima, Y., Ho, L. C., & Ptak, A. F. 2000a, *ApJ*, 539, 161
 Terashima, Y., Ho, L. C., Ptak, A. F., Mushotzky, R. F., Serlemitsos, P. J., Yaqoob, T., & Kunieda, H. 2000b, *ApJ*, 533, 729
 Tonry, J., Dressler, A., Blakeslee, J. P., Ajhar, E. A., Fletcher, A. B., Luppino, G. A., Metzger, M. R., & Moore, C. B. 2001, *ApJ*, in press (astro-ph/0011223)
 Townsley, L. K., Broos, P. S., Garmire, G. P., & Nousek, J. A. 2000, *ApJ*, 534, L139
 Tully, R. B. 1988, *Nearby Galaxies Catalog* (Cambridge: Cambridge Univ. Press)
 Ward, M. J., Done, C., Fabian, A. C., Tennant, A. F., & Shafer, R. A. 1988, *ApJ*, 324, 767
 Weisskopf, M. C., O'Dell, S. L., & van Speybroeck, L. P. 1996, *Proc. SPIE*, 2805, 2

⁸As these papers show, the $L_X-L_{H\alpha}$ correlation is not an artifact of distance effects.